XXI IMEKO World Congress "Measurement in Research and Industry"
August 30 – September 4, 2015, Prague, Czech Republic

CHARGE-TRANSFER-BASED SIGNAL INTERFACE FOR RESISTIVE SENSORS

Jorge E. Gaitán-Pitre, Ramon Pallas-Areny

Universitat Politècnica de Catalunya, BarcelonaTech (UPC), Castelldefels, Spain, ramon.pallas@upc.edu

Abstract – Charge transfer has been demonstrated to be a cost-effective method to measure capacitive sensors with low-end microcontrollers. Here we apply charge transfer to measure the output of voltage dividers that include a high-value resistive sensor hence extending the advantages of this method to a large group of sensors. By using two-point calibration, the maximal deviation obtained, referred to the Full Scale Span (FSS), is ±4 % for sensors between 100 kΩ and 1 MΩ, and ±5 % for sensors between 1 MΩ and 10 MΩ.

Keywords: Resistive sensor, charge transfer method, sensor-to-microcontroller interface, direct sensor interface

1. BASIC INFORMATION

Signal interfaces for resistive sensors are usually based on voltage divider circuits and derivatives thereof such as dc bridges and pseudo-bridges, or on sinusoidal or relaxation oscillators [1]–[4]. These circuits rely on either analogue components and analogue-to-digital converters (ADC) or time/frequency measurements [3], [4]. When applied to high-resistance sensors they include a circuit node that has a high-impedance to ground, which renders them susceptible to capacitive interference [1], [2] and may ask for electric shielding. Overall, the number of components hinders the design of cost-effective solutions based on these approaches.

Here we propose an interface circuit based on the charge-transfer method where the unknown resistance is calculated by counting the number of charge-transfer cycles needed to charge an integrating capacitor (C_r) to a threshold voltage (V_T) via a known sampling capacitor (C_s) and a voltage divider that includes a resistive sensor R_x. The operating principle is similar to that of switched capacitor circuits that implement resistors in microelectronic circuits [5], which suggests that the ability to reject external EMI here achieved may be similar to that of those microelectronic circuits.

Charge-transfer circuits can be implemented by a low-end microcontroller (MCU) as single active component [6]–[11], which makes them a cost-effective solution widely used in industrial applications, particularly in on/off detection systems such as touch screens. Their simplicity and cost reduction increase when the MCU does not need to include even a timer. This is in contrast to direct interfaces that rely on an MCU that includes an ADC [12]. In a previous work [8], we analysed the susceptibility of charge-transfer-based sensor interfaces for capacitive sensors to uncertainty sources such as stray capacitance and temperature and power supply voltage drifts, and proposed design solutions to reduce their effect. Here we aim to extend the advantages of those circuits to resistive sensors with values between 100 kΩ and 10 MΩ, which are a typical range, for example, for some NTC thermistors and light-dependent resistors (LDR).

2. DESCRIPTION AND ANALYSIS OF THE INTERFACE CIRCUIT PROPOSED

2.1. Operating principle

Fig. 1 shows the operating principle for resistance measurements based on the charge-transfer method. The procedure is similar to that proposed in [6]–[8] to measure capacitive sensors, but instead of charging an unknown capacitance (sensor) to a known voltage, a known sampling capacitor C_s is charged to the output voltage of a voltage divider that includes a resistive sensor R_x. R_r is a reference resistor, C_r is a known integrating capacitor much larger than C_s, V_S is a dc voltage, and S1, S2 and S3 are analogue switches. All component values are assumed to remain constant during a measurement cycle.

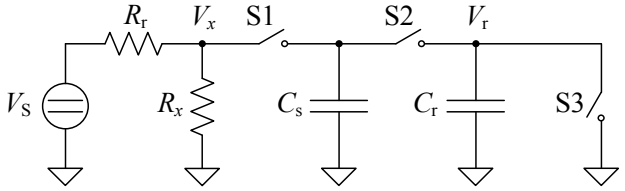

Fig. 1. Charge-transfer circuit to measure a sensor R_x. R_r is a reference resistor, C_s and C_r are known and $C_r >> C_s$.

The measurement method involves three stages: 1) Initial discharge of C_r and C_s at each new measurement; 2) Charging of C_s; and 3) charge transfer from C_s to C_r and counting the number of charge-transfer cycles required to reach a given voltage V_T across C_r ($V_r = V_T$). Initially, S1, S2, and S3 are open. In stage 1, S2 and S3 close, so that $V_r[0] = 0$ V. In stage 2, S2 and S3 open, and S1 closes hence C_s is charged towards V_x, the output voltage of the voltage divider, with a time constant $\tau = (R_x||R_r)C_s$. In stage 3, S1 opens and S2 closes, so that C_s and C_r are connected in parallel and the charge stored in them redistributes, which results in a voltage increment across C_r proportional to the charge transferred from C_s to C_r. By repeating stages 2 and 3, C_s exponentially charges C_r toward V_x. After N cycles, if the stage 2 lasts long enough for C_s to fully charge to V_x,

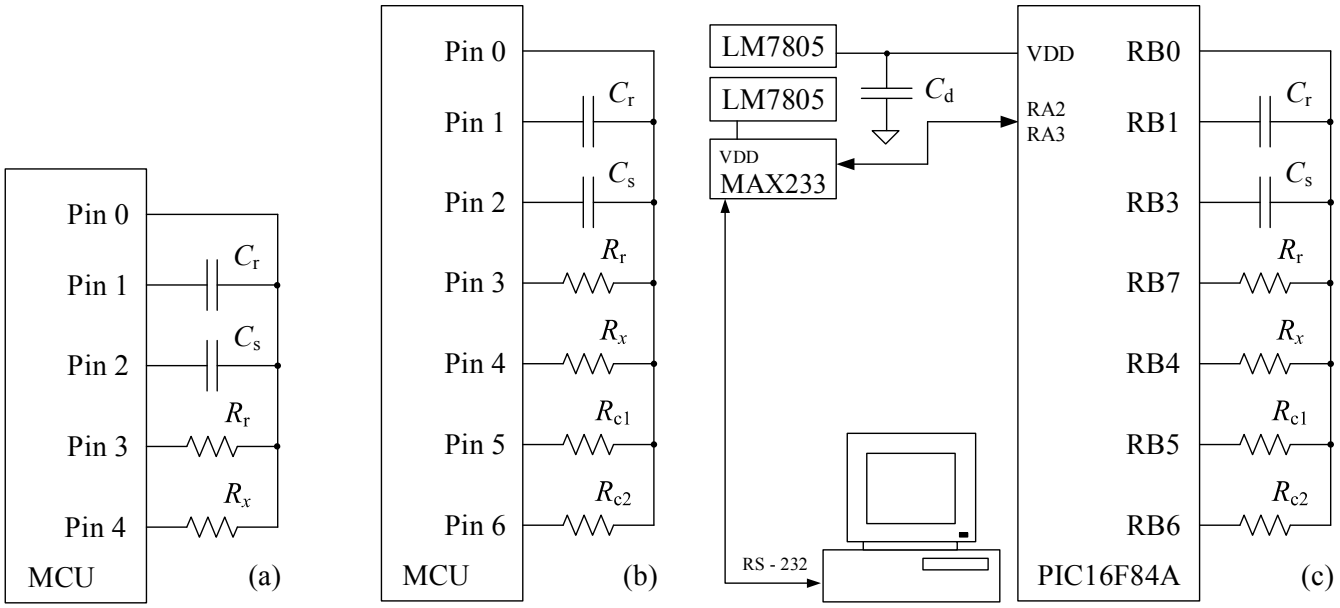

Fig. 2. Charge-transfer circuit to measure a resistive sensor R_x: (a) Basic circuit; (b) Circuit with two calibration resistors R_{c1} and R_{c2}. (c) Experimental setup to assess circuit performance. R_r is a reference resistor, and C_s and C_r are known capacitors.

the voltage across C_r at any arbitrary N charge-transfer cycle will be

$$V_r[N] = \frac{C_s}{C_s + C_r} V_x + \frac{C_r}{C_s + C_r} V_r[N-1] \qquad (1)$$

where $V_x = V_S R_x/(R_x + R_r)$. If $V_r0] = 0$ V because of the initial discharge stage, $C_r >> C_s$ and $V_x > V_T$, the number N of charge transfer cycles needed to charge C_r to a given threshold voltage V_T, i.e. $V_r[N] = V_T$, will be

$$N \approx \frac{C_r}{C_s} \ln\left(\frac{V_x}{V_x - V_T}\right) \approx \frac{C_r}{C_s}\left(\frac{V_T}{V_x} + \frac{V_T^2}{2V_x^2} + \frac{V_T^3}{3V_x^3} + \ldots\right). \qquad (2)$$

If, in a first approach analysis, only the first term of the series development in (2) is retained, we obtain

$$R_x \approx \frac{k}{N-k} R_r \qquad (3)$$

where $k = V_T C_r/V_S C_s$. The condition $V_x > V_T$ implies that R_r must be selected to fulfil the condition $R_r < R_{x,\min}(V_S/V_T - 1)$ where $R_{x,\min}$ is the minimal sensor resistance. This means that we need $V_S > V_T$. Since the resolution depends on N, if we select the limit value for R_r then for $R_{x,\min}$ we will obtain $N_{\min} = C_r/C_s$, hence we will also need $C_r >> C_s$. A smaller R_r value would yield a smaller $N_{\min}$.

2.2. Charge-transfer circuit implementation

Fig. 2(a) shows an implementation of the method in Fig. 1. The sensor is directly connected to an MCU without any intermediate electronics. Pins #0 to #4 of the MCU are digital input/output (I/O) pins. Generally, I/O pins can be configured according to one of three states: (a) LOW digital output ("0"), i.e. a voltage V_{OL} with an equivalent internal resistance R_{OL}; (b) HIGH digital output ("1"), i.e. a voltage V_{OH} with an equivalent internal resistance R_{OH}; and (c) INPUT, which offers high impedance (HZ).

Initially, pins #0 to #4 are set as inputs to avoid their unpredictably behaviour when turning on. Then, the three stages of the operating principle explained in the previous section are implemented. For the initial discharge, pins #0 and #1 are set as outputs that provide a "0" and C_r is discharged towards V_{OL}, with a time constant $\tau_D = 2R_{OL}C_r$. In order to charge C_s, pins #0 and #1 are set as inputs, whereas pins #2, #3 and #4 are set as outputs that respectively provide a "0", "1" and "0". C_s is charged towards V_x, with a time constant

$$\tau_C = \frac{\left(R_{x,\max} + R_{OL}\right)\left(R_r + R_{OH}\right)C_s}{\left(R_{x,\max} + R_{OL}\right) + \left(R_r + R_{OH}\right)} \qquad (4)$$

where $R_{x,\max}$ is the maximal sensor resistance. Finally, in the charge transfer stage, pins #0 and #2 remain in their previous state, pin #1 is set as an output that provides a "0", pins #3 and #4 are set as inputs, and the control program starts counting the number of charge transfer cycles; no timer is required. In this stage, part of the stored charge on C_s is transferred to C_r with a time constant $\tau_R = 2R_{OL}C_s$, and pin #0 act as a voltage threshold detector. The charging and charge-transfer stages are repeated until the voltage across C_r reaches the trigger level V_T of the input buffer. If we assume $V_{OL} \approx 0$ V, the initial discharging stage will leave no charge on C_s and C_r, and if $C_r >> C_s$, the number N_x of charge transfer cycles needed to charge C_r to V_T, i.e. $V_r[N_x] = V_T$, will be

$$N_x \approx \frac{C_r}{C_s} \ln\left(\frac{V_x}{V_x - V_T}\right) \qquad (5)$$

where $V_x = V_{OH}(R_x + R_{OL})/(R_x + R_r + R_{OL} + R_{OH})$. If we assume $V_{OL} \approx 0$ V and $C_r >> C_s$, we can approximate

$$R_x \approx \frac{R_{eq}}{N_x - k} k - R_{OL} \qquad (6)$$

where $R_{eq} = R_r + R_{OH}$ and $k = V_T C_r / V_{OH} C_s$. V_T and V_{OH} depend on the MCU power supply voltage, and R_{eq} and k depend, in addition, on temperature. Therefore, R_{OL} and R_{OH} contribute offset and sensitivity (gain) effects respectively. These dependences and contributions and, to some extent, the nonlinearity involved in (5), can be reduced by calibrating at two points, as described in [8], so that measurement results depend on the two reference resistors used for calibration rather than on the parameters above.

Each stage of the measurement process must last long enough to ensure that the final voltage across C_s and C_r is close enough to its ideal value. By waiting during ten time constants, i.e. $T_D > 10\tau_D$ for the discharging stage, $T_C > 10\tau_C$ for the charging stage, and $T_R > 10\tau_R$ for the charge-transfer stage, the relative deviation of the final voltage is less than 0.005 %. Furthermore, a long T_D reduces dielectric absorption effects in C_s and C_r [13].

2.3. Two-point calibration

Fig. 2(b) shows how to add two calibration resistors R_{c1} and R_{c2} to the circuit proposed in Fig. 2(a). The MCU now measures three resistances, R_x, R_{c1} and R_{c2} by applying the procedure in section 2.2. For R_x, pin #4 implements the tasks of pin #4 in Fig. 2(a), whereas pins #5 and #6 are set as HZ. For R_{c1} and R_{c2}, pins #5 and #6 implement the tasks of pin #4 in Fig. 2(a) respectively, whereas pins not involved in the measurement are configured as HZ. The number of charge transfer cycles required for each resistor (N_x, N_{c1}, N_{c2}) is given by (6), with the respective R_{OL} values. If we assume $R_{OL,4} \approx R_{OL,5} \approx R_{OL,6}$ and that k and R_{eq} remain constant during the calibration procedure, solving the equation system with the three N values yields

$$R_x \approx \frac{R_{c1} R_{c2} \left(N_{c1} - N_{c2} \right)}{R_{c1} \left(N_{c1} - N_x \right) - R_{c2} \left(N_{c2} - N_x \right)} \qquad (7)$$

which is independent of k hence of V_T, V_{OH}, C_r, C_s, and R_r.

R_{c1} and R_{c2} can be selected according to different criteria. If the measurement range is narrow enough, selecting them to be equal to 15 % and 85 % of the measurement span, respectively, minimizes the maximal deviation in the sense that the deviation at midrange will be equal to that at the range ends provided the transfer characteristic response curve is approximately quadratic [14].

3. EXPERIMENTAL SETUP

The measurement method proposed has been validated by implementing it with a MCU PIC16F84A connected to a 4 MHz crystal-oscillator, as shown in Fig. 2(c). The instruction cycle time was 1 µs. The PIC16F84A is a low-end MCU that does not include even a timer. The control program was written in assembler language. The function of pins #0, #1, #2, #3, #4, #5, and #6 were implemented by pins RB0, RB1, RB3, RB7, RB4, RB5 and RB6, respectively.

R_x was emulated by resistors from 100 kΩ to 10 MΩ in two subranges: 100 kΩ to 1 MΩ (range #1) and 1 MΩ to 10 MΩ (range #2), which are common values for some LDRs and NTC thermistors [1]. The temperature coefficient of the resistors was 700×10^{-6}/ºC for subrange #1 and 1500×10^{-6}/ºC for subrange #2. R_{c1} and R_{c2} were selected equal to 15 % and 85 % of the corresponding span. C_s was a 100 pF ceramic capacitor and C_r was 1,0 µF, with metalized polyester dielectric.

R_x, R_{c1}, and R_{c2} were measured with a digital multimeter (Agilent 34401), whose accuracy is better than ±(0,010 % Reading + 10 Ω) in the 1 MΩ range and ±(0,040 % Reading + 100 Ω) in the 10 MΩ ranges. C_s and C_r were measured with an impedance analyser (Agilent 4294A) connected to a test fixture (Agilent 16047E), which basic relative uncertainty is better than ±1 % from 1 pF to 1 nF, when measuring at 100 kHz and 0,5 V (rms oscillator output level). T_D, T_C, and T_R were calculated from the minimal R_{OL} and maximal R_{OH} values for pins RB0, RB1, RB3, RB7, RB4, RB5, and RB6, indirectly measured by the voltage-divider technique described in [2].

Each resistor was measured 25 times, hence obtaining 25 values for N_x, N_{c1}, and N_{c2}. These values were sent to a personal computer via a serial link (EIA-232) implemented with a MAX233 IC and the RA2 and RA3 MCU pins, under LabVIEW control. Next, we calculated 25 values of R_x by using (7), their mean $R_{x,av}$, and its deviation relative to the Full Scale Span (FSS), RD = $|R_x - R_{x,av}|$/FSS.

Measurement uncertainty was reduced by applying some design solutions proposed in [2] and [8]. External interference was reduced by configuring unused I/O pins of the MCU as inputs and connecting them to ground. Parasitic capacitance to ground was reduced by not using any ground plane in the printed circuit board. Although this may result in an increased capacitive interference, there was no need to use any conductive shield or any other method to reduce that interference in our busy laboratory environment. In order to reduce the effects of power supply noise, the MCU and MAX233 were each supplied by a separate voltage regulator (LM7805). Finally, a decoupling capacitor C_d = 100 nF was connected between the MCU power supply pin and ground as recommended by the manufacturer.

4. EXPERIMENTAL RESULTS AND DISCUSSION

Table 1 summarizes the experimental values of $R_{x,min}$ and $R_{x,max}$ for both measurement ranges, and the R_r value selected according to the measurement range. R_{OL} and R_{OH}, for pins RB0, RB1, RB3, RB7, RB4, RB5 and RB6 were below 50 Ω and 125 Ω, respectively. C_s was 99,21 pF, and C_r was 100,00 nF. Consequently, T_D and T_R should be larger than, 1,01 ms and 1,01 ns, respectively, and, from the experimental values shown in Table 1, T_C should be larger than 250 µs for subrange #1 and 2,5 ms for subrange #2. T_D was selected to be 10 ms to minimize any possible dielectric absorption effect in C_s and C_r [13]. T_R was selected to be 25 µs by considering the minimal number of instructions to execute at each stage of the charge-transfer measurement process. Table 1 also includes the values selected for T_C.

Table 1. $R_{x,min}$, $R_{x,max}$ and R_r for each measurements subrange.

Range	$R_{x,min}$ (MΩ)	$R_{x,max}$ (MΩ)	R_r (MΩ)	T_C (s)
1	0,09	1,00	0,22	3×10^{-6}
2	9,98	10,16	2,16	3×10^{-3}

Fig. 3 shows the experimental deviation relative to FSS (RD) for the two subranges. The maximal RD was ±4 %FSS from 100 kΩ to 1 MΩ [Fig. 3(a)], and ±5 %FSS from 1 MΩ

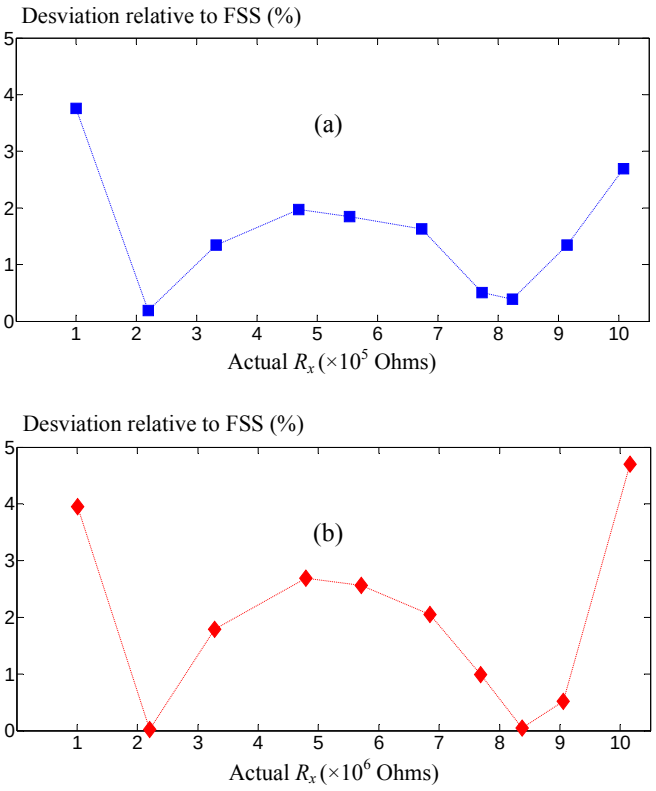

Fig. 3. Deviation relative to FSS for R_x between: (a) 100kΩ and 1 MΩ, and (b) 1MΩ and 10 MΩ.

to 10 MΩ [Fig. 3(b)]. The experimental results were very similar for both subranges, which suggests that the absolute deviation may be attributable to the nonlinearity of (5) and (6). RD was minimal when $R_x \approx R_{c1}$ and $R_x \approx R_{c2}$, and was maximal at the ends of the measurement range, as expected from the calibration resistors selected. Those relative deviations are acceptable in many industrial applications where cost is a major design constraint, such as in several automotive applications.

On the other hand, the algorithm used to calculate R_x makes the response independent from the reference resistor (R_r), the reference capacitors (C_s and C_r), MCU parameters, and their temperature dependence. Furthermore, the circuit does not require any electric shielding because capacitive interference is minimal in spite of the high-value resistors used.

5. CONCLUSIONS

A novel charge-transfer-based circuit to measure high-value resistive sensors has been proposed that can be implemented by low-end MCUs that do not need to include any ADC neither any timer, and three passive components: one resistor and two capacitors. The theoretical analysis shows the relevant parameters that determine the transfer characteristic of the resistance-to-digital conversion, which is nonlinear. The circuit has been experimentally tested by measuring resistors from 100 kΩ to 10 MΩ, divided in two subranges: 100 kΩ to 1 MΩ, and 1 MΩ to 10 MΩ. The use of two calibrating resistors for each subrange makes the response independent from MCU parameters, capacitors' values and their temperature dependence, and reduces the nonlinearity below ±5 %FSS.

ACKNOWLEDGMENTS

Jorge E. Gaitán-Pitre was supported by a joint-grant from Universitat Politècnica de Catalunya, BarcelonaTech (UPC) and SEAT Technical Centre. The authors would like to thank the Castelldefels School of Telecommunications and Aerospace Engineering (EEATC) for its research facilities and Mr. F. López for his technical support.

REFERENCES

[1] R. Pallàs-Areny and J. G. Webster, *Sensors and Signal Conditioning*, 2nd ed., John Wiley & Sons, New York, 2001.

[2] F. Reverter and R. Pallàs-Areny, *Direct Sensor-to-Microcontroller Interface Circuits: Design and Characterisation*, Marcombo, Barcelona, 2005.

[3] N. M. Mohan, B. George, and V. J. Kumar, "A novel dual-slope resistance-to-digital converter," *IEEE Trans. Instrum. Meas.*, vol. 59, no. 5, pp. 1013–1018, May 2010.

[4] J. H.-L. Lu, M. Inerowicz, S. Joo, J.-K. Kwon, and B. Jung, "A low-power, wide-dynamic-range semi-digital universal sensor readout circuit using pulsewidth modulation," *IEEE Sens. J.*, vol. 11, no. 5, pp. 1134–1144, May 2011.

[5] P. E. Allen and E. Sánchez-Sinencio, *Switched Capacitor Circuits*, Van Nostrand Reinhold, New York, 1984.

[6] P. H. Dietz, D. Leigh, and W. S. Yerazunis, "Wireless liquid level sensing for restaurant applications," in *Proceedings of IEEE Sensors*, pp. 715–720, vol. 1, Orlando, Florida, Jun. 2002.

[7] H. Philipp, "Charge transfer capacitance measurement circuit," US6466036B1, 15-Oct-2002.

[8] J. E. Gaitán-Pitre, M. Gasulla, and R. Pallàs-Areny, "Analysis of a direct interface circuit for capacitive sensors," *IEEE Trans. Instrum. Meas.*, vol. 58, no. 9, pp. 2931–2937, September 2009.

[9] S. Kim, W. Choi, W. Rim, Y. Chun, H. Shim, H. Kwon, J. Kim, I. Kee, S. Kim, S. Lee, and J. Park, "A highly sensitive capacitive touch sensorintegrated on a thin-film-encapsulated active-matrix OLED for ultrathin displays," *IEEE Trans. Electron Devices*, vol. 58, no. 10, pp. 3609–3615, October 2011.

[10] H. Philipp, "Touch sensitive control panel," US7969330B2, 28-Jun-2011.

[11] J. K. Reynolds and K. Hargreaves, "Methods and systems for sigma delta capacitance measuring using shared components," US7977954B2, 12-Jul-2011.

[12] G.A.M. Nastasi, A. Scuderi, H.-E. Endres, W. Hell, and K. Bock, "Simple cost effective and network compatible readout for capacitive and resistive (chemical) sensors," *Procedia Eng.*, vol. 87, pp. 1234–1238, 2014.

[13] J. C. Kuenen and G. C. M. Meijer, "Measurement of dielectric absorption of capacitors and analysis of its effects on VCO's," *IEEE Trans. Instrum. Meas.*, vol. 45, no. 1, pp. 89–97, February 1996.

[14] R. Pallàs-Areny, J. Jordana, and Ò. Casas, "Optimal two-point static calibration of measurement systems with quadratic response," *Rev. Sci. Instrum.*, vol. 75, no. 12, pp. 5106–5111, December 2004.